

(6Mepy)₃tren]²⁺ (Table II, Figure 6). Upon conversion to high-spin [Fe(6Mepy)₃tren]²⁺ there is a decrease in the number of electrons in π orbitals (Figure 5) and a further increase in the Fe-N_{im} bond distance.¹³ Both of these effects lead to decreased metal-ligand interaction, and the imine stretching frequency increases another 23 cm⁻¹ (Figure 6).

Conclusions

Raman spectroscopy is a sensitive technique for accurately determining the imine stretching frequency in low-spin Fe(II) α -diimine complexes. This is due, at least in part, to the low-energy MLCT transitions of these compounds that lead to resonance Raman enhancement as the exciting frequency approaches that of the MLCT.⁶ This special sensitivity is illustrated by [Fe(PMI)₃]²⁺, for which previous assignments⁴ of the imine stretch based on infrared spectra were incorrect. It is further demonstrated by the Raman spectrum of [Fe-(6Mepy)₃tren]²⁺ for which both the high- and low-spin forms are observed at room temperature. This represents the first time that the low-spin species has been observed at room temperature. It seems likely that this technique should be applicable to other metal-imine systems that contain metals such as Cu(I), Cr(0), and Ru(II) in lower oxidation states and in which the imine stretches appear to have unusual behavior on the basis of infrared spectroscopy.³⁰⁻³²

Although the actual amounts of electron delocalization from metal to α -diimine π^* orbitals are not known, the trends in imine stretching frequency allow a qualitative evaluation of the importance of π delocalization and some of the factors affecting it. For all of the complexes in this study, it is most extensive with low-spin Fe(II), where there are the maximum number of electrons available for donation and the highest metal-ligand overlaps. Even then, the imine stretches are still in the region expected for double bonds, indicating that the overall changes in N_{im}-C_{im} bond strength are relatively small.

Acknowledgment. Support provided through Grant CHE74-19328A02 from the National Science Foundation is gratefully acknowledged.

Registry No. [Fe(BMI)₃](PF₆)₂, 85828-60-0; [Ni(BMI)₃](PF₆)₂, 85828-62-2; [Fe(PMI)₃](PF₆)₂, 36487-65-7; [Co(PMI)₃](PF₆)₂, 36465-55-1; [Mn(py)₃tren](PF₆)₂, 85828-68-8; [Fe(py)₃tren](PF₆)₂, 55222-32-7; [Co(py)₃tren](PF₆)₂, 63526-13-6; [Ni(py)₃tren](PF₆)₂, 56348-41-5; [Cu(py)₃tren](PF₆)₂, 85828-64-4; [Zn(py)₃tren](PF₆)₂, 85828-66-6; [Fe(6Mepy)₃tren](PF₆)₂, 55190-36-8; [Ni-(6Mepy)₃tren](PF₆)₂, 56348-47-1.

(30) Gagné, R. R.; Ingle, D. M.; Lisensky, G. C. *Inorg. Chem.* **1981**, *20*, 1991.

(31) King, R. B.; Douglas, W. M. *J. Am. Chem. Soc.* **1973**, *95*, 7528.

(32) Lane, B. C.; Lester, J. E.; Basolo, F. *J. Chem. Soc. D* **1971**, 1618.

Contribution from the Departments of Chemistry, University of Washington, Seattle, Washington 98195, and Trinity University, San Antonio, Texas 78284

Laser Raman Spectroscopic Studies of Metal α -Diimine Complexes. 2. Studies of a Spin-Equilibrium System

WILLIAM H. BATSCHELET*¹ and N. J. ROSE

Received September 22, 1982

Raman spectroscopy was used to differentiate between high- and low-spin Fe(II) in [Fe(6Mepy)₃tren]²⁺ spin-crossover systems on the basis of differences in the imine stretching region (1600-1700 cm⁻¹). The spin equilibria of the complex in solution and in the solid state as PF₆⁻, BF₄⁻, and BPh₄⁻ salts were studied. The spin crossovers are adequately described by using a Boltzmann distribution between two states with an incomplete transition occurring for the BPh₄⁻ salt. Factors affecting the equilibria are discussed, and an explanation of the discrepancies between the Raman data and other physical measurements is given in terms of resonance-Raman enhancement of the low-spin Fe(II) imine band and the nucleation and growth mechanism of phase transitions in solids.

Introduction

Octahedral and pseudooctahedral transition-metal complexes having d⁴-d⁷ configurations exist in either high-spin or low-spin electronic ground states, depending on the nature of the ligating atoms. For a relatively small number of complexes, the properties of the ligands are such that the energy differences between the high- and low-spin states are on the order of kT . The result is a spin crossover or spin equilibrium, and a number of spin-crossover systems and their properties have been reviewed.²⁻⁸

For compounds having spin crossovers, the fraction of molecules in the high-spin state decreases with decreasing temperature, often with a dramatic transition from high to low spin occurring over a few degrees. In addition, incomplete transitions to fully low-spin (residual paramagnetism) or fully high-spin states have been observed in which the ratio of high- to low-spin molecules reaches a plateau.^{2,3} Various models have been proposed to explain these phenomena,^{2,3} and recently Hendrickson and co-workers⁹⁻¹¹ used the nucleation and growth mechanism of phase transitions^{12,13} in solids to explain

(1) Trinity University.

(2) Güttlich, P. *Struct. Bonding (Berlin)* **1981**, *44*, 83.

(3) Goodwin, H. A. *Coord. Chem. Rev.* **1976**, *18*, 293.

(4) Martin, R. L.; White, A. H. *Transition Met. Chem. (N.Y.)* **1968**, *4*, 113.

(5) Barefield, E. K.; Busch, D. H.; Nelson, S. M. *Q. Rev., Chem. Soc.* **1968**, *22*, 457.

(6) König, E. *Coord. Chem. Rev.* **1968**, *3*, 471.

(7) Sacconi, L. *Pure Appl. Chem.* **1971**, *27*, 161.

(8) König, E. *Ber. Bunsenges. Phys. Chem.* **1972**, *76*, 975.

(9) Haddad, M. S.; Federer, W. D.; Lynch, M. W.; Hendrickson, D. N. *J. Am. Chem. Soc.* **1980**, *102*, 1470.

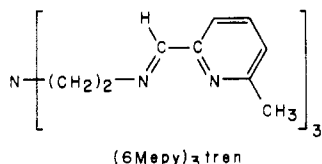
(10) Haddad, M. S.; Lynch, M. W.; Federer, W. D.; Hendrickson, D. N. *Inorg. Chem.* **1981**, *20*, 123.

(11) Haddad, M. S.; Federer, W. D.; Lynch, M. W.; Hendrickson, D. N. *Inorg. Chem.* **1981**, *20*, 131.

(12) Rao, C. N. R.; Rao, K. J. "Phase Transitions in Solids"; McGraw-Hill: New York, 1978.

these effects in some Fe(III) complexes.

The complexes in this study are the $[\text{Fe}(\text{6Mepy})_3\text{tren}]\text{X}_2$ series



where $\text{X} = \text{PF}_6^-$, BF_4^- , and BPh_4^- . These were originally synthesized by Wilson¹⁴ and have subsequently been investigated by a variety of techniques.¹⁴⁻¹⁸ All previous evidence indicated that $[\text{Fe}(\text{6Mepy})_3\text{tren}](\text{PF}_6)_2$ was exclusively high spin at room temperature, and there was no evidence for a spin equilibrium occurring in solution.¹⁵ However, the room-temperature Raman spectra of this compound indicate the simultaneous presence of both the high- and low-spin forms in the solid state and in solution.^{19,20} Vibrational spectroscopy has previously been used in studies of spin-crossover systems, typically by identifying infrared bands corresponding to the high- and low-spin states and then using these bands as spin-state markers.^{2,3,6,21,22} Because we could observe the presence of both spin states, we have investigated the spin equilibria of $[\text{Fe}(\text{6Mepy})_3\text{tren}]\text{X}_2$ systems using variable-temperature Raman spectroscopy in the hope that a more complete understanding of the factors influencing spin transitions could be obtained.

The following work is the first use of Raman spectroscopy to systematically monitor a spin-equilibrium system known to the authors.

Experimental Section

Compounds. All reagents were obtained commercially and were used without further purification. All solvents were reagent grade.

$[\text{Fe}(\text{6Mepy})_3\text{tren}](\text{PF}_6)_2$ was prepared and recrystallized according to literature methods¹⁵ by using NH_4PF_6 in place of KPF_6 .

$[\text{Fe}(\text{6Mepy})_3\text{tren}]\text{X}_2$ ($\text{X} = \text{BF}_4^-$, BPh_4^-). **Method A.** The BF_4^- and BPh_4^- salts were prepared by substituting the appropriate NaX salt for KPF_6 in the literature preparation of $[\text{Fe}(\text{6Mepy})_3\text{tren}](\text{PF}_6)_2$.¹⁵ The BF_4^- salt was recrystallized from a 1:1 v/v acetonitrile/ether solution.

Method B. The BF_4^- and BPh_4^- salts were also prepared by metathesis of $[\text{Fe}(\text{6Mepy})_3\text{tren}](\text{PF}_6)_2$. LiBr in acetone was added to acetone solutions of the PF_6^- salt, resulting in the formation of a dark red oil. The oil was washed with acetone and dissolved in methanol, and methanol solutions of the appropriate NaX salt were added. The $[\text{Fe}(\text{6Mepy})_3\text{tren}](\text{BPh}_4)_2$ precipitated immediately, and $[\text{Fe}(\text{6Mepy})_3\text{tren}](\text{BF}_4)_2$ was precipitated by the addition of ethanol such that the final methanol:ethanol ratio was approximately 1:2 v/v. Infrared spectra of samples from either method of preparation were indistinguishable, and the only differences in the infrared spectra of the various salts were due to the differences in anion absorption peaks.

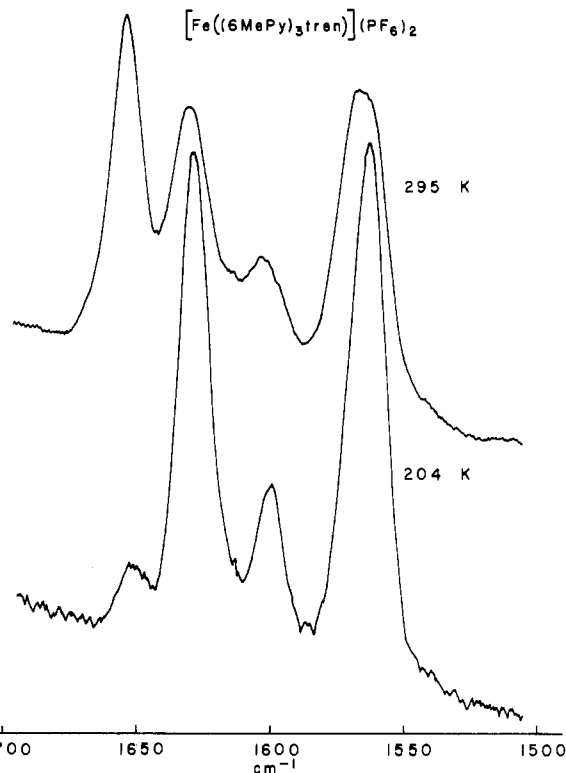


Figure 1. Temperature dependency of the Raman spectrum of solid $[\text{Fe}(\text{6Mepy})_3\text{tren}](\text{PF}_6)_2$.

There was no evidence in the infrared spectra for acetone, methanol, or ethanol molecules of solvation.

Physical Measurements. Infrared spectra of the solids were recorded with a Beckman IR 10 spectrophotometer.

Raman spectra were obtained with the instrumentation previously described.¹⁹ Solid samples were powdered and placed in capillary tubes, which were placed in a brass sample holder. This was then suspended inside a double-walled quartz tube, which had a flat bottom and an inlet on one side near the bottom. Nitrogen was admitted through the inlet; it flowed around the sample and escaped out at the top of the tube. By regulation of the temperature of the nitrogen, the temperature of the sample could be controlled. Liquid samples were placed in a flat-bottom quartz cell containing approximately 0.5 mL. This cell was in turn suspended inside the double-walled tube. The temperature of the solid samples was monitored by a copper-constantan thermocouple inserted directly into the capillary tube and placed just above the incident laser beam. For liquid samples, the thermocouple was placed inside a solvent-filled capillary tube, which was then inserted into the sample cell. A minimum of 20 min was allowed for equilibration between temperatures, and spectra were not recorded until the thermocouple reading was constant. The 568.2-nm Kr^+ line was used as the exciting frequency (λ_{ex}) for all samples. In addition, some data were collected with use of the 514.5-nm Ar^+ and 647.1-nm Kr^+ lines.

Results

As shown in Figure 3 of ref 19, the room-temperature Raman spectrum of solid $[\text{Fe}(\text{6Mepy})_3\text{tren}](\text{PF}_6)_2$ is unique among the $[\text{M}(\text{py})_3\text{tren}](\text{PF}_6)_2$ and $[\text{M}(\text{6Mepy})_3\text{tren}](\text{PF}_6)_2$ complexes in that it has two distinct peaks in the 1615–1670- cm^{-1} region. The peak at 1652 cm^{-1} is assigned as the imine stretch of high-spin $[\text{Fe}(\text{6Mepy})_3\text{tren}](\text{PF}_6)_2$ while that at 1629 cm^{-1} is assigned to the low-spin complex. This assignment is supported by variable-temperature Raman spectroscopy as shown in Figure 1 for solid $[\text{Fe}(\text{6Mepy})_3\text{tren}](\text{PF}_6)_2$. The peak corresponding to the imine stretch of the low-spin form is seen to increase in intensity with decreasing temperature while that assigned to the high-spin species decreases. This assignment has been independently confirmed by low-temperature infrared spectroscopy.¹⁶ The simultaneous presence of both the high- and low-spin species at room tem-

- (13) Christian, J. W. "The Theory of Transformations in Metals and Alloys", 2nd ed.; Pergamon Press: Oxford, 1975; Part I.
- (14) Wilson, L. J. Ph.D. Thesis, University of Washington, Seattle, WA, 1971.
- (15) Hoselton, M. A.; Wilson, L. J.; Drago, R. S. *J. Am. Chem. Soc.* **1975**, *97*, 1722.
- (16) Delker, G. L. Ph.D. Thesis, University of Illinois, Urbana-Champaign, IL, 1976.
- (17) Wilson, L. J.; Georges, D.; Hoselton, M. A. *Inorg. Chem.* **1975**, *14*, 2968.
- (18) Lazarus, M. S.; Hoselton, M. A.; Chou, T. S. *Inorg. Chem.* **1977**, *16*, 2549.
- (19) Batschelet, W. H.; Rose, N. J. *Inorg. Chem.*, preceding paper in this issue.
- (20) Batschelet, W. H.; Rose, N. J. "Abstracts of Papers", 172nd National Meeting of the American Chemical Society, San Francisco, CA, Aug 1976; American Chemical Society: Washington, DC, 1976; INOR 201.
- (21) Hutchinson, B.; Neill, P.; Finkelstein, A.; Takemoto, J. *Inorg. Chem.* **1981**, *20*, 2000.
- (22) Czernuszewicz, R. S.; Nakamoto, K.; Strommen, D. P. *Inorg. Chem.* **1980**, *19*, 793.

Table I. Raman Imine Stretching Frequencies for $[\text{Fe}(\text{6Mepy})_3\text{tren}]\text{X}_2^a$

X state	BF_4^- solid	PF_6^- solid	BPh_4^- solid	BF_4^- soln in acetonitrile	PF_6^- soln in acetone
high-spin freq	1656	1652	1651	1657	1656
low-spin freq	1631	1629	1629	1631	1631

^a Peak locations given in cm^{-1} ; uncertainty $\pm 1 \text{ cm}^{-1}$.

perature was also observed for the BF_4^- and BPh_4^- salts and for solutions of $[\text{Fe}(\text{6Mepy})_3\text{tren}]^{2+}$ in acetone or acetonitrile, and temperature-dependent Raman spectra were recorded for all of these systems.

The success of Raman spectroscopy in detecting the presence of low-spin $[\text{Fe}(\text{6Mepy})_3\text{tren}]^{2+}$ is due in part to the resonance-Raman effect. The complex has an intense metal-to-ligand charge-transfer band at 568 nm,¹⁶ and excitation in that region leads to enhanced Raman intensity for vibrational modes associated with the chromophoric unit, including the imine stretch, as has been shown for related low-spin Fe(II) complexes.^{19,22,23} Consistent with this, the relative peak intensities of the high- and low-spin forms vary with the exciting frequency, but in all cases, both imine stretches can be observed at room temperature. The relative imine peak intensities also show a dependence on the anion or physical state (vide infra), but the peak locations are essentially constant (Table I). Since the only temperature-dependent term in the expression for Raman intensity is $[1 - \exp(-h\nu/kT)]^{-1}$,²⁴ temperature effects in the range 100–300 K are negligible for frequencies in the 1600- cm^{-1} range, and the Raman intensity should be a temperature-independent measure of the number of complexes exhibiting that band. Allowing each spin state to have its own Raman intensity proportionality constant (C) leads to the expression for $R(\text{HS}/\text{LS})$ given in eq 1.

$$R(\text{HS}/\text{LS}) = C_{\text{HS}}N_{\text{HS}}/C_{\text{LS}}N_{\text{LS}} \quad (1)$$

$$R(\text{HS}/\text{LS}) = \frac{\text{high-spin imine peak intensity}}{\text{low-spin imine peak intensity}}$$

N = the number of complexes in each state

The relative peak intensities for calculating $R(\text{HS}/\text{LS})$ were determined with a Du Pont 310 curve resolver programmed for Gaussian peaks. There are three imine moieties per $(\text{6Mepy})_3\text{tren}$ ligand that can couple in the idealized C_3 symmetry of the complex and yield two Raman-active bands (A and E modes). The imine stretching region of a spectrum of $[\text{Fe}(\text{6Mepy})_3\text{tren}]^{2+}$ in acetonitrile that has been curve resolved is shown in Figure 2. The two peaks labeled Py arise from the pyridine groups,¹⁴ and those labeled HS and LS arise from the imine stretches of high- and low-spin $[\text{Fe}(\text{6Mepy})_3\text{tren}]^{2+}$, respectively. The results of the acetonitrile solution with $R(\text{HS}/\text{LS})$ determined by total peak area ratio or by major peak area ratio (the ratio determined by using only the higher energy imine stretch for each species) are indistinguishable. However, the major peak area ratios were used for the least-squares analysis of the data since they were less sensitive to overlap with neighboring peaks, especially in cases of low peak intensity. The values of $R(\text{HS}/\text{LS})$ varied smoothly as a function of temperature for all samples. They were reproducible for both cooling and warming cycles, and there were no signs of hysteresis. Furthermore, within experimental uncertainty, the value of $R(\text{HS}/\text{LS})$ did not vary as a function

$[\text{Fe}(\text{6Mepy})_3\text{tren}](\text{BF}_4)_2$ in CH_3CN 232 K

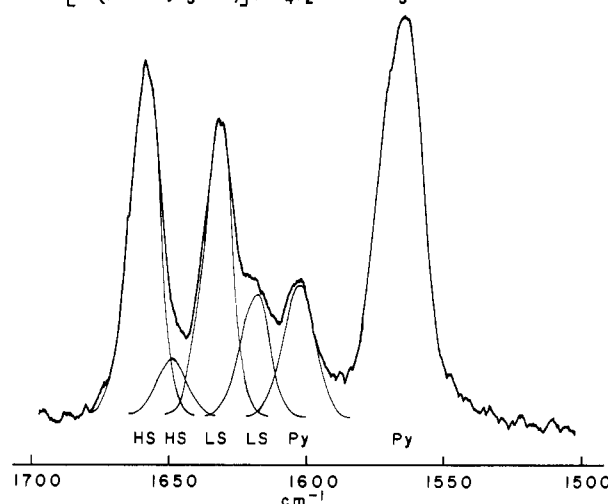


Figure 2. Curve-resolved spectrum of $[\text{Fe}(\text{6Mepy})_3\text{tren}]^{2+}$ in acetonitrile.

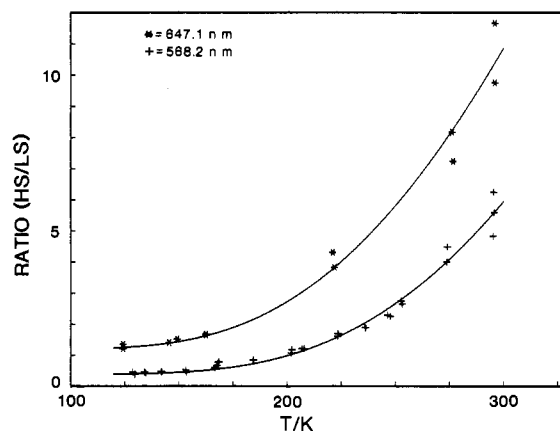


Figure 3. $R(\text{HS}/\text{LS})$ vs. temperature for solid $[\text{Fe}(\text{6Mepy})_3\text{tren}](\text{BPh}_4)_2$; +, $\lambda_{\text{ex}} = 568.2 \text{ nm}$; *, $\lambda_{\text{ex}} = 647.1 \text{ nm}$. The solid lines are least-squares fits.

of the length of time that a sample was at a particular temperature.

Discussion

The model used to describe the spin equilibria in this work is a modified Boltzmann distribution given in eq 2, in which

$$R(\text{HS}/\text{LS}) = A \exp(-E/RT) + B \quad (2)$$

a constant (B) representing incomplete transition to the low-spin form is included. Although the ${}^5\text{T}(\text{O}_h)$ high-spin state should be split into ${}^5\text{A}$ and ${}^5\text{E}$ states by the C_3 symmetry of the $(\text{6Mepy})_3\text{tren}$ ligand, only a single high-spin state separated by an energy gap (E) from the low-spin state is included. Previous work on $[\text{Fe}(\text{6Mepy})_3\text{tren}]^{2+}$ ^{15,17} and similar systems^{2,25} has shown that the ${}^5\text{E}$ state is on the order of 800–1000 cm^{-1} higher than the ${}^5\text{A}$ state, and any contribution to $R(\text{HS}/\text{LS})$ by the ${}^5\text{E}$ state should be negligible over the temperature range in this study.²⁶

The results of least-squares analyses²⁷ using eq 2 are summarized in Table II. Within experimental uncertainty, the value of B is 0 for all members of the series except solid

- (23) (a) Clark, R. J. H.; Turtle, P. C.; Strommen, d. P.; Streusand, B.; Kincaid, J.; Nakamoto, K. *Inorg. Chem.* **1977**, *16*, 84. (b) Streusand, B.; Kowal, A. T.; Strommen, D. P.; Nakamoto, K. *J. Inorg. Nucl. Chem.* **1977**, *39*, 1767.
(24) Woodward, L. A. "Raman Spectroscopy"; Szymanski, H. A., Ed.; Plenum Press: New York, 1967.

(25) Chum, H. L.; Vanin, J. A.; Holanda, M. I. D. *Inorg. Chem.* **1982**, *21*, 1146.

(26) It was possible to fit the data by using a double exponential function; however, the differences between the preexponential terms were several orders of magnitude, which seemed physically unrealistic.

(27) "Program BMDP3R—Nonlinear Regression, BMDP Biomedical Computer Programs"; University of California Press: Los Angeles, CA, 1981.

Table II. Least-Squares Fit for $[\text{Fe}(\text{6Mepy})_3\text{tren}]X_2$ Spin Equilibria Using $R(\text{HS/LS}) = A \exp(-E/RT) + B^a$

X	A	E, kJ/mol	B^b	T, K ^c	$R(\text{HS/LS})_{\text{calcd}}^d$	$R(\text{HS/LS})_{\text{obsd}}^d$
BF_4^- solid	192 (48)	14.0 (0.6)	0.40	201–318	0.67	0.66
PF_6^- solid	144 (28)	11.8 (0.5)		132–324	1.23	1.22
BPh_4^- solid	491 (100)	11.2 (0.5)		129–296	5.74	5.56
BF_4^- in acetonitrile	779 (224)	12.3 (0.7)		232–298	5.44	5.40
PF_6^- in acetone	244 (41)	8.8 (0.4)		185–299	7.00	7.40

^a $\lambda_{\text{ex}} = 568.2$ nm; standard deviations are given in parentheses. ^b Restricted values; see text for explanation. ^c Temperature range of study. ^d $R(\text{HS/LS})$ at 298 K.

Table III. Dependency of Solid $[\text{Fe}(\text{6Mepy})_3\text{tren}]X_2$ Spin Equilibria on Exciting Frequency^a

X	λ_{ex} , nm	A	E_{av} , kJ/mol	B^b	$R(\text{HS/LS})_{\text{calcd}}^c$	$R(\text{HS/LS})_{\text{obsd}}^c$
BF_4^-	568.2	202 (4)	14.1 (0.9)	0.40	0.68	0.66
	647.1	385 (10)			1.30	1.35
	514.6	351 (9)			1.18	1.16
BPh_4^-	568.2	323 (9)	10.2 (0.8)	0.36 (0.05)	5.62	5.56
	647.1	587 (20)		1.20	10.76	10.70

^a Standard deviations are given in parentheses. ^b Restricted values; see text for explanation. ^c $R(\text{HS/LS})$ at 298 K.

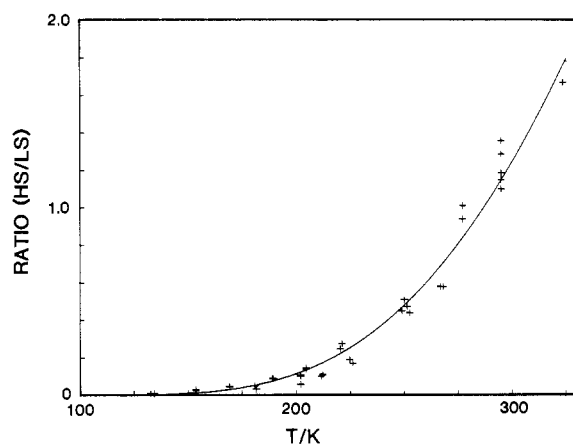


Figure 4. $R(\text{HS/LS})$ vs. temperature for solid $[\text{Fe}(\text{6Mepy})_3\text{tren}](\text{PF}_6)_2$. The solid line is the least-squares fit.

$[\text{Fe}(\text{6Mepy})_3\text{tren}](\text{BPh}_4)_2$, which has a high degree of residual paramagnetism ($\mu_{\text{eff}} = 4.3 \mu_{\text{B}}$ at 86 K).¹⁵ The value of B was subsequently limited to less than or equal to the minimum in $R(\text{HS/LS})$ for the BPh_4^- salt and was fixed at 0 for the rest of the series, and the data in Table II were obtained under these restrictions. Also given in Table II are the temperature ranges at which the equilibria were studied and the values of $R(\text{HS/LS})$ at 295 K observed and calculated from the least-squares data.

As seen in Figures 3–5, eq 2 successfully describes the spin equilibria over the entire temperature range. Figure 3 also shows the effect of changing the exciting frequency. Because of the resonance-Raman effect, the values of $R(\text{HS/LS})$ are dependent upon the exciting frequency (eq 1, 2). However, least-squares fits for exciting frequencies other than 568.2 nm for the BPh_4^- and BF_4^- salts as solids do not yield values of E significantly different from those given in Table II. Table III summarizes the results of least-squares fits for these anions using average values of E . In both cases the value of $R(\text{HS/LS})$ decreases by a factor of approximately 1.9 on going from an exciting frequency of 647.1 to 568.2 nm due to the resonance-Raman-enhanced intensity of the low-spin form as the exciting frequency approaches the maximum in its electronic transition.

Focusing on the trend in E for the $[\text{Fe}(\text{6Mepy})_3\text{tren}]X_2$ series (Table II), one sees that E decreases in the solid state as the anion size increases. This is reflected in the values of $R(\text{HS/LS})$ (Table II) and in the magnetic moments of these salts. The BPh_4^- salt has the highest values of $R(\text{HS/LS})$ and

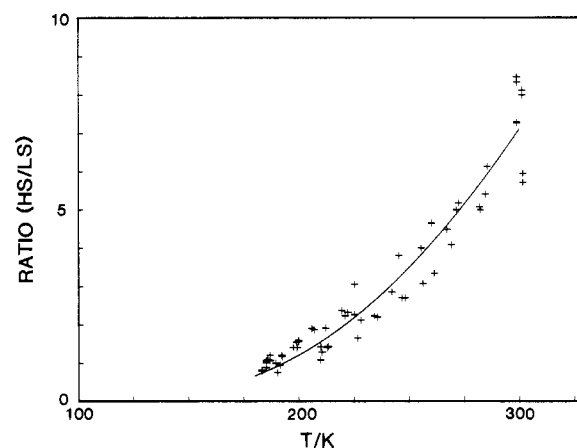


Figure 5. $R(\text{HS/LS})$ vs. temperature for $[\text{Fe}(\text{6Mepy})_3\text{tren}](\text{PF}_6)_2$ in acetone solution. The solid line is the least-squares fit.

room-temperature magnetic moment ($5.41 \mu_{\text{B}}$) while the BF_4^- salt has the lowest ($5.21 \mu_{\text{B}}$).²⁸ Thus, as noted for this^{15,16} and other systems,^{2,3} lattice effects clearly play a role in spin equilibria. The arms of the $(\text{6Mepy})_3\text{tren}$ ligand open upon conversion to the high-spin form,^{15,16} and the trend in E may represent the ease in undergoing this change. The BF_4^- salt, which presumably has the smallest lattice and would be the most difficult for the arms to expand against, has the highest value of E while the BPh_4^- salt, which should have the largest lattice and be the easiest to move against, has the lowest E .

In solution where there are no lattice forces, the $[\text{Fe}(\text{6Mepy})_3\text{tren}]^{2+}$ complex still exhibits a spin equilibrium with relatively small values of E and high values of $R(\text{HS/LS})$. The differences between the acetonitrile and acetone solvent systems are attributed to solvent effects, as have been observed for similar systems.^{2,15,25,29} These represent the differences in the solvation of the complex by the two solvents and the fact that there must be reorganization of the solvent cage following spin state transition.

Equation 2 can be used to evaluate the thermodynamic parameters associated with the low-spin \rightleftharpoons high-spin equilibrium since $R(\text{HS/LS}) = \alpha K_{\text{eq}}$, where α is a constant incorporating the Raman intensity proportionality constants. As

- (28) Magnetic susceptibilities were determined by the Faraday technique using a Cahn RG electrobalance and a Varian Associates V-4005 4-in. electromagnet with $\text{HgCo}(\text{SCN})_4$ as the calibrant. Diamagnetic corrections were determined from the corresponding $[\text{Zn}(\text{py})_3\text{tren}]X_2$ salt.
 (29) Reeder, K. A.; Dose, E. V.; Wilson, L. J. *Inorg. Chem.* **1978**, *17*, 1071.

Table IV. Thermodynamic Parameters for the Spin Equilibria of $[\text{Fe}(\text{6Mepy})_n(\text{py})_m](\text{PF}_6)_2^a$

compd	ΔH° , kJ/mol	ΔS° , J/mol K	ref
	Solid		
(6Mepy) ₃ tren	11.8 (0.5)	41 (2) ^b	this work
	20.2 (7.8)	87 (38)	15
(6Mepy) ₂ (py)tren	13.0 (1.0)	41 (3)	15
(6Mepy)(py) ₂ tren	20.0 (1.0)	41 (3)	15
	Solution		
(6Mepy) ₃ tren in acetonitrile	12.3 (0.7)	55 (2) ^b	this work
in acetone	8.8 (0.4)	46 (1) ^b	this work
(6Mepy) ₂ (py) in acetone/Me ₂ SO	11.9 (1.6)	36 (6)	15
(6Mepy)(py) ₂ in acetone/Me ₂ SO	19.2 (13.7)	42 (39)	15

^a Standard deviations are given in parentheses. ^b $\Delta S^\circ_{\text{min}}$.

a result, $\Delta H^\circ = E$ and $\Delta S^\circ = R \ln A - R \ln \alpha$ for cases where $B = 0$. Assuming $C_{\text{LS}} \geq C_{\text{HS}}$ (eq 1) leads to $\alpha \leq 1$ and $\Delta S^\circ_{\text{min}} = R \ln A$, where $\Delta S^\circ_{\text{min}}$ is the minimum entropy change associated with the spin transition. The results for the PF_6^- salt are summarized in Table IV along with the previous results of Hoselton et al. for this and the closely related $[\text{Fe}(\text{6Mepy})_n(\text{py})_m\text{tren}](\text{PF}_6)_2$ compounds.¹⁵ The thermodynamic parameters determined by Raman spectroscopy are consistent with those previously obtained from magnetic susceptibility measurements and provide further evidence that the energy difference between the low- and high-spin states decreases as the number of methyl groups on the (6Mepy)_n(py)_mtren ligand increases.^{15,17}

Attempts to correlate the Raman spin-equilibrium measurements with temperature-dependent magnetic susceptibility experiments were not successful in reproducing the rather sharp transition from high to low spin for the PF_6^- and BF_4^- salts.^{15,16} This failure is most likely due to the intrinsic differences between the two measurements. Magnetic susceptibility reflects the bulk properties of a sample while Raman spectroscopy measures the properties of a finite number of molecules in a small region near the surface.

Various models have been suggested to account for the nature of spin-crossover systems.^{2,3} Sorai and Seki³⁰ suggested

that there is cooperative behavior involving domains (groups of molecules) that simultaneously undergo a spin transition. The larger the domain size, the greater the degree of cooperativity and the sharper the transition.

Recently Hendrickson and co-workers⁹⁻¹¹ have used the nucleation and growth mechanism of phase transitions in solids^{12,13} to account for the degree of sharpness in the transition as well as incomplete transitions and the sensitivity of spin-crossover systems to solvation and sample preparation. According to this mechanism, phase transformations can be broken down into two processes. The first is nucleation in which small regions (domains) of transformed molecules are produced by fluctuations in the parent phase. Preferred sites for the formation of domains are crystal defects such as grain boundaries, vacancies, and impurities. Before a domain can continue to exist, it has to exceed a minimum critical size. Subsequent growth of the transformed phase requires the transfer of molecules from the parent phase onto the product phase at the boundaries of the domain. Kinetics controls both the rate of nucleation and the velocity of the phase transformation.^{12,13} Using the nucleation and growth mechanism, Hendrickson and co-workers⁹⁻¹¹ were able to explain the behavior of some Fe(III) spin-crossover complexes that were systematically ground and/or doped into complexes not undergoing spin-state transitions.

The nucleation and growth mechanism also accounts for the behavior of the complexes in this paper and for the discrepancies between the Raman data and previous measurements.¹⁴⁻¹⁶ Since it is primarily a surface phenomenon, Raman spectroscopy focuses on the preferred region for the formation of low-spin domains. In this region, it appears that a Boltzmann distribution is sufficient to describe the ratio between high- and low-spin complexes, just as it does in solution. Only for the solid BPh_4^- salt, which has a high degree of residual paramagnetism,¹⁵ is modification to account for incomplete transition required. The data in Tables II and IV then reflect the nucleation portion of the phase transformation and say nothing about the growth of low-spin domains.

Acknowledgment. Support provided through Grant CHE74-19328A02 from the National Science Foundation is gratefully acknowledged. The support of Trinity University for the computer fitting is also appreciated (W.H.B.).

Registry No. $[\text{Fe}(\text{6Mepy})_3\text{tren}]^{2+}$, 55190-35-7; $[\text{Fe}(\text{6Mepy})_3\text{tren}](\text{PF}_6)_2$, 55190-36-8; $[\text{Fe}(\text{6Mepy})_3\text{tren}](\text{BF}_4)_2$, 85781-40-4; $[\text{Fe}(\text{6Mepy})_3\text{tren}](\text{BPh}_4)_2$, 85781-41-5.

(30) Sorai, M.; Seki, S. *J. Phys. Chem. Solids* 1974, 35, 555.